S. J. Lewis

Regression Model for LPE Film Property Control

Abstract: Empirical regression equations permit the calculation of liquid phase epitaxial (LPE) film properties from film growth parameters. Numerical differentiation of these equations facilitates examination of the sensitivities of film properties to fluctuations in growth conditions and the development of depletion-compensating growth strategies. Regression equations for nominal 3-μm bubble size CaGe and Ga films have been generated and used for quantitative comparisons of the growth behavior of the two systems. A real time feedback control scheme has been applied to the Ga system resulting in 70 percent of the as-grown films falling within ± 1 percent of the target collapse field.

Introduction

Liquid phase epitaxial (LPE) garnet films are usually grown from $PbO\text{-}B_2O_3$ fluxed melts of the garnet constituents. In the isothermal dipping technique [1], the garnet substrates are most often supported horizontally and rotated to ensure rapid establishment of a steady state boundary layer at the growth interface. The properties of films grown in this manner depend in a very complicated way on the melt composition, growth rate, growth temperature, and film thickness. To be able to predict, quantitatively, the film properties from the growth conditions, one must have detailed knowledge of melt constituent segregation coefficients, lattice site occupancies, and dependence of film magnetic properties on composition and crystal structure. The theory as it now exists [1–17] provides understanding of the various relationships, but it is not quantitative to the degree necessary to control the growth process to the tight tolerances required in a multichip module manufacturing scheme. Such a scheme must be able to quickly compensate for deviations in film properties due to melt changes, melt depletion, temperature measurement inaccuracies, and numerous other irregularities.

A regression model has been developed which quantitatively describes film properties as functions of the growth parameters. These equations are empirical and, therefore, do not provide the insights to be gained from a theoretical understanding of the relationships. They do, however, permit quantitative evaluation of the effect of process changes on film properties and enable multi-variable growth strategies to be devised easily.

Regression analysis

A regression equation can be written to relate empirically the film growth parameters to the film properties. The literature on LPE film growth [9, 10, 18–20] shows that plots of saturation magnetization, M_s, versus growth rate and versus various melt compensation ratios, R values [3], are linear over wide ranges of the parameter values. The slopes of the linear curves depend on the other R values. This type of behavior can be described by regression equations involving only the experimental variables and their first order interactions. In addition, work in this laboratory shows that growth rate, g, characteristic length, ℓ, wall energy, σ_w, anisotropy field H_k, anisotropy, K_u, quality factor, Q, exchange constant, A, lattice mismatch, Δa, and minimum drive field, H_c, can all be described by these main effects-first order interaction regression equations. Table 1 lists, for $(EuYTm)_3(FeGa)_5O_{12}$, the adjustable growth conditions and some corresponding film properties.

The model considers only the thickness-independent properties. The thickness-dependent properties can then be derived by including the growth time.

The generalized regression equation which describes the relationship between properties and parameters has the form

$$Y_i = C_{0,i} + C_{1,i}X_1 + C_{2,i}X_2 + \cdots + C_{n,i}X_n + C_{1,2,i}X_1X_2 + \cdots + C_{j,k,i}X_jX_k + \cdots + C_{(n-1),n,i}X_{(n-1)}, X_n \quad \text{for} \quad k > j,$$

Table 1 Adjustable growth conditions and corresponding film properties.

Growth parameters (independent variables)		*Film properties (dependent variables)*	
	Thickness-independent		
T_g	(growth temperature)	g	(growth rate)
ω	(substrate rotation rate)	M_s	(magnetization)
$R_{F/G}$	$\left(\frac{Fe_2O_3}{Fe_2O_3 + Ga_2O_3}\right)$	ℓ	(characteristic length)
R_{Tm}	$(Tm_2O_3/\Sigma Ln_2O_3)$	σ_W	(wall energy)
R_{Sm}	$(Sm_2O_3/\Sigma Ln_2O_3)$	H_k	(anisotropy field)
$R_{F/L}$	$\left(\frac{Fe_2O_3}{\Sigma Ln_2O_3}\right)$	K_u	(anisotropy)
R_Σ	$\left(\frac{\Sigma Ln_2O_3 + Fe_2O_3 + Ga_2O_3}{1/2\ P_BO + B_2O_3 + Top}\right)$	Q	(quality factor)
R_{Pb}	$\left(\frac{P_BO}{2B_2O_3}\right)$	A	(exchange constant)
		Δa	(lattice mismatch)
		μ	(mobility)
		V_p	(peak velocity)
		H_c	(minimum drive field)
		T_s	(saturation temperature)
	Thickness-dependent		
t	(time)	H_o	(collapse field)
		w_s	(stripe width)
		h	(thickness)

where the C_i are empirically determined constants, the Y_i are the measured properties, and the X_i are the growth parameters. The number n is the total number of parameters considered. There will be a similar equation for each of the i properties. The number of constants in the equation and, therefore, the number of different films which must be grown to solve for them is given by

$$\text{minimum number of films} = \frac{(n+1)n}{2} + 1.$$

The computation scheme used generates an equation for growth rate in terms of T_g, $\sqrt{\omega}$, and the appropriate R ratios. Temperature T_g, g, and the R ratios are then used as independent variables to generate equations for the other thickness-independent properties. Finally, M_s, ℓ, and time t are used to generate the thickness-dependent properties. This results in a set of equations in which the thickness-independent properties are described as functions of the absolute growth temperature, T_g, the rotation rate, ω, and the melt composition (R ratios). The thickness-dependent properties have, in addition, a dependence on the time for growth, t. These equations can be used to calculate the film properties, or given a set of film properties they can be solved for the growth conditions. The values obtained, however, are very sensitive to systematic differences in temperature measurement between

Table 2 Equations used in model.

$$g = C_{0g} + C_{1g}T_g + C_{2g}\sqrt{\omega} + C_{12g}T_g\sqrt{\omega} \quad \text{(references [2] and [9])}$$

$$M_s = C_{0M} + C_{1M}T_g + C_{2M}g + C_{12M}T_g g$$

$$\ell = C_{0\ell} + C_{1\ell}T_g + C_{2\ell}g + C_{12\ell}T_g g, \text{ etc.}$$

$$H_o = H_o(M_s, \ell, h) \quad \text{(reference [22])}$$

$$w_s = w_s(\ell, h) \quad \text{(reference [21])}$$

$$h = g\ t$$

$$\frac{\partial H_o}{\partial x} = \left.\frac{\partial H_o}{\partial M_s}\right)_{\ell,h} \left.\frac{\partial M_s}{\partial x}\right)_{\substack{\text{growth}\\ \text{conditions}}} + \frac{\partial H_o}{\partial \ell}\frac{\partial \ell}{\partial x} + \frac{\partial H_o}{\partial h}\frac{\partial h}{\partial g}\frac{\partial g}{\partial x}$$

$$\frac{\partial w_s}{\partial x} = \frac{\partial w_s}{\partial \ell}\frac{\partial \ell}{\partial x} + \frac{\partial w_s}{\partial h}\frac{\partial h}{\partial g}\frac{\partial g}{\partial x}$$

$$\frac{\partial h}{\partial x} = \frac{\partial h}{\partial g}\frac{\partial g}{\partial x},$$

where $x = t_g$ or ω and $\frac{\partial h}{\partial g} = t$

$$\frac{\partial H_o}{\partial t} = \frac{\partial H_o}{\partial h}\frac{\partial h}{\partial t}$$

$$\frac{\partial w_s}{\partial t} = \frac{\partial w_s}{\partial h}\frac{\partial h}{\partial t}$$

$$\frac{\partial h}{\partial t} = g$$

Table 3 Samples of $(Eu,Y,Tm)_3(Fe,Ga)_5O_{12}$ used to generate equations.

ω (rpm)	T_g (°C)	g (μm/min)	M_s (T × 10^4)[a]	ℓ (μm)	σ_w (10^7J/cm^2)[b]	H_c $\left(\frac{4\pi\cdot A\cdot m^{-1}}{1000}\right)$[c]
100.0000	963.0	1.60	261.5	0.379	0.206	0.38
200.0000	963.2	1.70	322.7	0.370	0.306	0.27
200.0000	974.7	0.76	261.4	0.426	0.232	0.43
100.0000	973.9	0.49	256.7	0.466	0.244	0.34
150.0000	974.9	0.77	277.2	0.440	0.269	0.26
250.0000	974.9	1.01	273.0	0.412	0.244	0.15
150.0000	960.3	1.52	320.1	0.380	0.310	0.12
250.0000	960.1	1.96	305.1	0.356	0.263	0.21

[a]Numbers can be read directly in gauss.
[b]Numbers can be read directly in ergs/cm².
[c]Numbers can be read directly in oersteds.

different growth stations and to slight differences in composition between supposedly identical melts. The derivatives of the film properties with respect to T_g and ω are much less sensitive to small variations in melt composition. For example, it has been found experimentally that the derivatives of the properties with respect to T_g and ω are relatively insensitive to small perturbations in the Fe/Ga ratio. This is because the terms involving T_g or ω interactions with melt ratios are small and the derivatives calculated are still valid when small melt adjustments are made. The equations are thus most useful when used in a difference mode in which the calculated properties are referred to those of a sample film grown from a particular melt in a particular growth station. Derivatives of the thickness-independent properties can be obtained numerically from the regression equations. They can then be combined (via the chain rule for partial derivatives) with numerical derivatives obtained from the equations of Fowlis and Copeland [21] and of Thiele [22], to generate derivatives of the thickness-dependent properties. The set of equations used for the simple case where the melt composition is fixed is listed in Table 2. The calculations are done in generalized form by an APL program in a computer.

Generation of regression equations

The film growth conditions are varied in a factorial manner to generate the number of points required to solve for the constants in the generalized regression equation. More points than the minimum are advisable so that a least squares solution can be made. The high and low levels of the parameters should be as far apart as possible to minimize the effects of measurement error and experimental scatter on the derived constants. Table 3 lists the experimental data for a $(Eu,Y,Tm,)_3(FeGa)_5O_{12}$ composition which was used to generate the regression constants. The data were taken in the order listed in the table in an attempt to randomize depletion effects (or any other systematic drift in growth conditions) over rotation rate and growth temperature. The Ga data in the table show a systematic drift in saturation temperature with time due to the small melt size used. Similar data were generated for a $(Sm,Y,Lu,Ca)_3(FeGa)_5O_{12}$ composition. The CaGe data show better reproducibility because of the use of a larger melt size. The derivatives generated at a typical set of growth conditions are listed in Tables 4 and 5 for the Ga and CaGe systems, respectively. The derivatives for the Ga system may be somewhat in error because of the large melt depletion effect. Although the actual derivatives may not be exactly correct, it is believed that the trends observed are accurate and that the general conclusions drawn are valid. These derivatives allow comparison of the sensitivities of film properties to growth conditions for the two systems.

Figure 1 is a plot of M_s vs growth rate as calculated from the regression equations. The actual experimental data are also plotted on the figure. Experiment and the regression fit agree within the measurement error.

Derivatives were also generated when films were grown with an oscillatory rotation (washing machine motion). The rotation speed in this case is the maximum rotation speed during the cycle. The derivatives for this motion are listed in Table 6 and are seen to be very similar to the values obtained for unidirectional rotation.

Comparison of Ga and CaGe systems

Examination of the sensitivities of the properties to growth parameters for the CaGe and Ga compositions shows a few important differences. First, M_s in the Ga system is a much stronger function of rotation than that in the CaGe system. Secondly, the effect of T_g on M_s (and collapse field H_0) in the two systems has the opposite

Table 4 Derivatives for $(Eu,Y,Tm)_3(Fe,Ga)_5O_{12}$. Growth conditions were 198 rpm at 964.7°C for 1.42 min. Properties were M_s = 0.0298 T, ℓ = 0.396 μm, and h = 2.22 μm.

	$\left.\frac{\partial}{\partial \omega}\right)_{T_g, t}$ (rpm⁻¹)	$\left.\frac{\partial}{\partial T_g}\right)_{\omega, t}$ (°C⁻¹)	$\left.\frac{\partial}{\partial t}\right)_{T_g, \omega}$ (min⁻¹)
g (μm/min)	0.0023	-0.0693	
M_s(T × 10^4)[a]	0.1469	-3.3291	
ℓ(μm)	-0.0002	0.0041	
σw (10^7J/cm²)[b]	0.0001	-0.0033	
H_c (4π·A·m⁻¹/1000)[c]	-0.0008	0.0084	
H_o (4π·A·m⁻¹/1000)[c]	0.2035	-5.2931	50.4406
w_s (μm)	-0.0004	-0.0011	0.4282
h (μm)	0.0032	-0.0984	1.5634

[a]Numbers can be read directly in gauss.
[b]Numbers can be read directly in ergs/cm².
[c]Numbers can be read directly in oersteds.

Table 5 Derivatives for $(Y,Sm,Lu,Ca)_3(Fe,Ge)_5O_{12}$ with unidirectional rotation. Growth conditions were 100 rpm at 915.5°C for 2.417 min. Properties were M_s = 0.0357 T, ℓ = 0.355 μm, and h = 1.95 μm.

	$\left.\frac{\partial}{\partial \omega}\right)_{T_g, t}$ (rpm⁻¹)	$\left.\frac{\partial}{\partial T_g}\right)_{\omega, t}$ (°C⁻¹)	$\left.\frac{\partial}{\partial t}\right)_{T_g, \omega}$ (min⁻¹)
g (μm/min)	0.0028	-0.0421	
M_s(T × 10^4)[a]	-0.0537	6.0891	
ℓ (μm)	0.0003	-0.0161	
σw (10^7J/cm²)[b]	0.0002	-0.0034	
H_o (4π·A·m⁻¹/1000)[c]	0.1946	1.9162	35.6384
w_s (μm)	0.0038	-0.1292	0.2164
h (μm)	0.0067	-0.1017	0.8089

[a]Numbers can be read directly in gauss.
[b]Numbers can be read directly in ergs/cm.
[c]Numbers can be read directly in oersteds.

sign, and the magnitude of $\partial H_0/\partial T_g$ for CaGe is smaller than for Ga. Finally, $\partial w_s/\partial T_g$ for Ga is much less than for CaGe. Otherwise the sensitivities of properties to parameters in both systems are of similar magnitude. These observations have implications for the ability to control collapse field and stripe width for the two compositions studied.

The collapse field derivative equations, listed in Table 2, involve three terms, one depending on magnetization, one on characteristic length, and one on film thickness. Similarly, $\partial w_s/\partial x$ has two terms, one involving ℓ and the other h. Table 7 lists the values of these terms for the two systems. In the CaGe system there is a self-compensating mechanism for collapse field. A positive temperature fluctuation causes M_s to increase and ℓ to decrease, both of which cause an increase in H_0. The same fluctuation, however, causes h to decrease, producing a compensating decrease in H_0. In fact, it is possible to choose film properties and growth conditions so that $\partial H_0/\partial T_g \approx 0$ for CaGe. The stripe width is not self-compensated. In the Ga system, the self-compensating mechanism operates on stripe width rather than on collapse field. This apparent

Figure 1 M_s vs growth rate for $(Y,Sm,Lu,Ga)_3(Fe,Ge)_5O_{12}$ with unidirectional rotation.

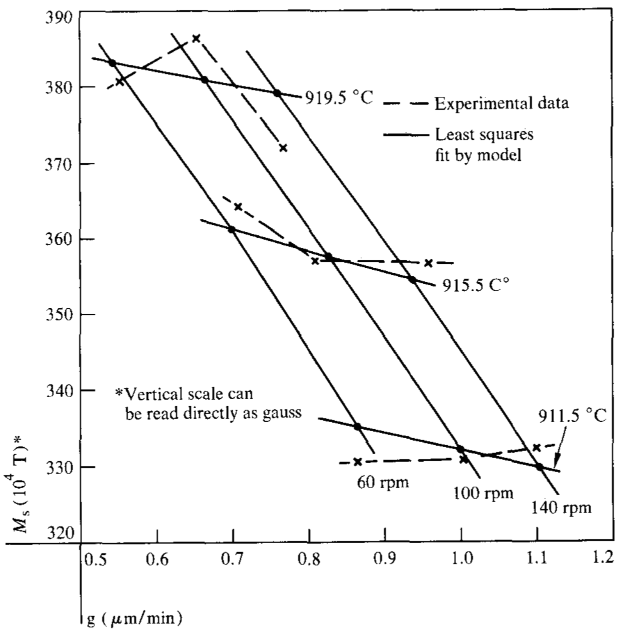

Table 6 Derivatives for $(Y,Sm,Lu,Ca)_3(Fe,Ge)_5O_{12}$ with oscillatory rotation. Growth conditions were 100 rpm at 915.5°C for 2.417 min. Properties were $M_s = 0.0357$ T, $\ell = 0.365$ μm, and $h = 1.88$ μm.

	$\left.\frac{\partial}{\partial \omega}\right)_{T_g, t}$ (rpm^{-1})	$\left.\frac{\partial}{\partial T_g}\right)_{\omega, t}$ (°C^{-1})	$\left.\frac{\partial}{\partial t}\right)_{T_g, \omega}$ (min^{-1})
g (μm/min)	0.0021	−0.0422	
M_s (T × 10^4)[a]	−0.0027	5.5930	
ℓ (μm)	0.0002	−0.0164	
σw (10^{7}J/cm^2)[b]	0.0002	−0.0043	
H_0 ($4\pi\cdot$A$\cdot$m^{-1}/1000)[c]	0.1781	1.3606	36.1732
w_s (μm)	0.0028	−0.1306	0.1849
h (μm)	0.0051	−0.1020	0.7758

[a]Numbers can be read directly in gauss.
[b]Numbers can be read directly in ergs/cm.
[c]Numbers can be read directly in oersteds.

Table 7 Expansion of temperature derivatives. When the equations in [21, 22] are differentiated, the following relations hold: $(\partial H_0/\partial M_s) > 0$, $(\partial H_0/\partial \ell) < 0$, $(\partial H_0/\partial h) > 0$, $(\partial w_s/\partial \ell) > 0$, and $(\partial w_s/\partial h) > 0$. Units are consistent with those used in previous tables.

		$\frac{\partial}{\partial M_s}\left(\frac{\partial M_s}{\partial T_g}\right)$	$\frac{\partial}{\partial \ell}\left(\frac{\partial \ell}{\partial T_g}\right)$	$\frac{\partial}{\partial h}\left(\frac{\partial h}{\partial g} \cdot \frac{\partial g}{\partial T_g}\right)$	*Sum*
CaGe	$\frac{\partial H_0}{\partial T_g}$	2.49	3.91	−4.48	1.92
	$\frac{\partial w_s}{\partial T_g}$		−0.102	−0.027	−0.129
Ga	$\frac{\partial H_0}{\partial T_g}$	−1.36	−0.74	−3.17	−5.27
	$\frac{\partial w_s}{\partial T_g}$		0.026	−0.27	0.001

disadvantage of Ga systems can be overcome by the use of a real time feedback control scheme during the film growth to compensate for temperature errors by changing the rotation rate.

Rotation compensation for temperature errors

In the LPE growth process, temperature can be measured more quickly than it can be changed, whereas the rotation rate can be changed almost instantaneously. This suggests a dynamic growth control scheme in which errors in the desired growth temperature are compensated by real time changes in the rotation rate, with the aim of keeping collapse field constant. Kasai and Ishida [23] report a similar scheme in which the run to run rotation rate is changed to keep growth rate constant in the face of temperature drifts. The system described here makes within-run changes in rotation rate to keep collapse field constant.

The amount of rotation compensation required can be calculated from the derivatives in Tables 4 or 5. In order to keep collapse field constant,

$$\frac{\partial H_0}{\partial T_g} \Delta T_g = -\frac{\partial H_0}{\partial \omega} \Delta\omega,$$

where ΔT_g is the temperature error and $\Delta\omega$ is the amount of rotation compensation needed. For the Ga system studied,

$$\frac{\Delta\omega}{\Delta T_g} = 26 \text{ rpm/deg C}.$$

Further examination of the derivatives for Ga shows that the change in ω required to keep collapse field constant also acts to closely compensate film thickness. This is because the bulk of the collapse field change for Ga is due to growth rate variation, and the compensation, therefore, works to keep growth rate constant. The stripe width dependence on both T_g and ω is small so the stripe width variation produced by this compensation scheme is negligible.

For the CaGe system, the situation is different. The same collapse field compensation scheme can be applied, but here a positive temperature error causes an increase in collapse field, which must be compensated by a decrease in rotation rate. This further reduces the thickness, which is already low because of the higher than desired temperature. Collapse field compensation with this CaGe composition thus operates by adjusting the film thickness. The stripe width variation with temperature is relatively large so the compensation scheme results in larger errors in stripe width than in the Ga system.

In summary, the CaGe system exhibits a self-compensating mechanism to correct collapse field for temperature errors, but film thickness and stripe width vary. In the Ga system, a feedback control scheme is possible which compensates both thickness and collapse field and causes insignificant variation in stripe width. This feedback control scheme has been realized with a process control computer and has been applied to the Ga system. The results show good compensation even when intentionally large temperature errors are introduced.

Development of growth strategies

With each film grown, there is a depletion of garnet constituents in the melt, which changes the properties of the next film grown. Hewitt, et al. [24] and Kasai and Ishida [23] report a depletion compensation scheme in which temperature and time are changed a fixed amount with each film grown to keep collapse field and film thickness within specified limits. Sumner and Cox [25] describe a scheme in which the sensitivities of characteristic length and growth rate to changes in temperature are determined for each melt. These derivatives are then used to correct for run to run shifts of characteristic length and growth rate.

The derivatives of Tables 4 and 5 can be used to develop a growth strategy for keeping collapse field, stripe width, and film thickness within specified boundaries. To do this the following equations must be solved simultaneously:

$$-\Delta H_{\mathrm{o\,dep}} = \frac{\partial H_{\mathrm{o}}}{\partial\omega}\,\Delta\omega + \frac{\partial H_{\mathrm{o}}}{\partial T_g}\,\Delta T_g + \frac{\partial H_{\mathrm{o}}}{\partial t}\,\Delta t,$$

$$-\Delta w_{\mathrm{s\,dep}} = \frac{\partial w_{\mathrm{s}}}{\partial\omega}\,\Delta\omega + \frac{\partial w_{\mathrm{s}}}{\partial T_g}\,\Delta T_g + \frac{\partial w_{\mathrm{s}}}{\partial t}\,\Delta t,$$

$$-\Delta h_{\mathrm{dep}} = \frac{\partial r}{\partial\omega}\,\Delta\omega + \frac{\partial r}{\partial T_g}\,\Delta T_g + \frac{\partial h}{\partial t}\,\Delta t$$

where $\Delta\omega$, ΔT_g, and Δt are the changes in growth parameters required to compensate all three properties for depletion effects, and $\Delta H_{\mathrm{o\,dep}}$, $\Delta w_{\mathrm{s\,dep}}$, and Δh_{dep} are the depletion effects (film$_n$-film$_{n-1}$). These depletion corrections can then be added to corrections calculated to compensate for errors in the properties of the previous film grown. The error corrections are calculated by replacing Δ_{dep} with the deviation from desired properties in the above equations. In practice, time and rotation rate can be changed more easily than temperature because of the long time constants of the LPE furnaces. The preferred strategy is, therefore, to compensate the two most rapidly varying film properties by changing ω and t with each film grown. When any of the properties drifts out of specification limits or when ω or t take on unacceptable values, then T_g is also varied to bring all properties back into range. When growth temperature changes can no longer bring about the desired effects, melt additions must be made to restore the melt to its undepleted condition. New sets of derivatives and revised growth strategies must be calculated periodically as growth conditions change.

Application to $(Eu,Y,Tm)_3(Fe,Ga)_5O_{12}$ film production

An automated growth control station was set up which included computer control of furnace temperature to ±0.2°C of setpoint, real time rotation compensation for temperature errors (based on collapse field), melt surface detection so growth always occurs at a fixed distance below the melt surface, and computer timing and sequencing of the growth process. Regression equations for an $(Eu,Y,Tm)_3(FeGa)_5O_{12}$ melt were determined from data generated with a melt of small size, but similar composition, in an offline furnace. A series of 81 films were grown over a period of five weeks from a 1500-gram production melt. No additions of garnet were made to the melt, but PbO was periodically added to maintain saturation temperature. Films were grown one at a time with three films grown between remelt cycles. Derivative calculations were used to adjust the growth conditions for each film based on the properties of the previous film and depletion estimations. Rotation rate and growth time were the parameters most often adjusted. The data reported cover all films grown from this melt, including four films grown ini-

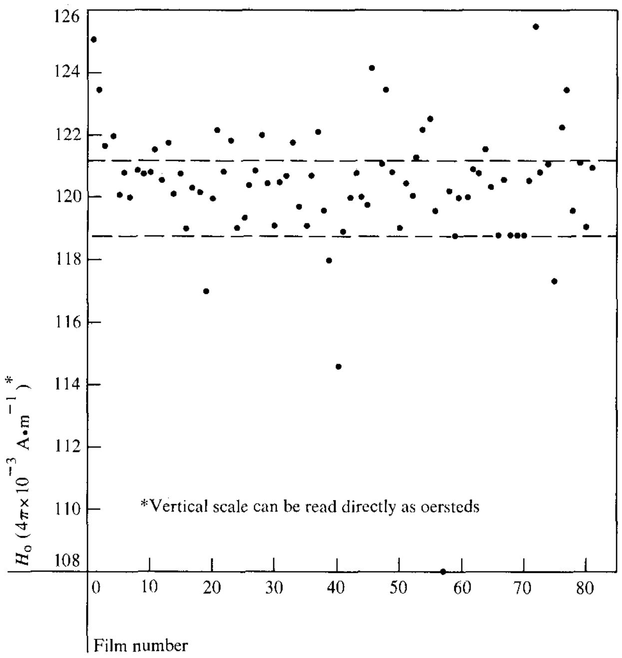

Figure 2 Collapse field vs film number for $(Eu,Y,Tm)_3(Fe,Ga)_5O_{12}$.

tially to determine saturation temperature, five films grown when there were computer or mechanical problems, and 14 films grown when the melt was seriously depleted in PbO. No lead oxide was available for replenishment. Of these 23 films grown under adverse conditions, 15 were outside the collapse field specification of 120 ± 1.2 Oe (9600 ± 96 A·m^{-1}). The overall collapse field yield for the as-grown films, including the above 23 films, was 70 percent. All films which met the collapse field specification also met thickness and stripe width specifications. The growth times for these 81 films ranged between 90 and 105 seconds, the growth temperatures between 966.9°C and 975.7°C, and the rotation rates between 100 and 130 rpm. The collapse field data are plotted in Fig. 2.

Conclusions

An empirical regression model for the LPE growth process allows quantitative determination of the sensitivities of all film properties to growth conditions. The sensitivities determined from this model permit quantitative comparison of the ease of controlling the properties of CaGe and Ga garnets. Although CaGe films exhibit self compensation for collapse field, the growth of Ga films should be more reproducible when real time feedback control of collapse field is used. The property derivatives determined from the regression equations allow feedback growth strategies designed to compensate for melt depletion to be determined easily.

Acknowledgments

The author thanks R. Atkin for suggesting the area of investigation and H. Turk and J. Davies for their interest in and support of this work and for helpful discussions clarifying the differences between CaGe and Ga systems. Without the experimental efforts of S. Guerriero, A. Cherry, J. Suits, and W. McChesney in providing the data required to develop the regression equations and to verify their predictive ability, this work could not have been completed.

References

1. H. J. Levinstein, S. Licht, R. W. Landorf, and S. Blank, *Appl. Phys. Lett.* **19,** 486 (1971).
2. E. A. Giess, J. D. Kuptsis, and E. A. D. White, *J. Cryst. Growth* **16,** 36 (1972).
3. S. L. Blank and J. W. Nielsen, *J. Cryst. Growth* **17,** 302 (1972).
4. E. A. Giess, B. E. Argyle, D. C. Cronemeyer, E. Klokholm, T. R. McGuire, D. F. O'Kane, T. S. Plaskett, and V. Sadagopan, *American Institute of Physics Conference Proceedings*, No. 5, 110 (1971).
5. W. Tolksdorf, G. Bartels, G. P. Espinosa, P. Holst, D. Nateika, and F. Welz, *J. Cryst. Growth* **17,** 322 (1972).
6. E. A. Giess, D. C. Cronemeyer, R. Ghez, E. Klokholm, and J. D. Kuptsis, *J. Amer. Ceram. Soc.* **56,** 593 (1973).
7. B. F. Stein, *American Institute of Physics Conference Proceedings*, No. 18, 48 (1973).
8. B. F. Stein and R. M. Josephs, *American Institute of Physics Conference Proceedings*, No. 10, 329 (1972).
9. S. L. Blank, B. S. Hewitt, L. K. Shick, and J. W. Nielsen, *American Institute of Physics Conference Proceedings*, No. 10, 256 (1972).
10. J. E. Davies, E. A. D. White, and J. D. C. Wood, *J. Cryst. Growth* **27,** 227 (1974).
11. S. L. Blank, F. B. Hagedorn, C. D. Brandle, and J. W. Nielsen, *IEEE Trans. Magnetics* **MAG-10,** 484 (1974).
12. J. M. Robertson, W. Tolksdorf, and H. D. Jonker, *J. Cryst. Growth* **27,** 241 (1974).
13. J. C. Brice, J. M. Robertson, W. T. Stacy, and J. C. Verplanke, *J. Cryst. Growth* **30,** 66 (1975).
14. J. M. Robertson, M. J. G. van Hout, and J. C. Verplanke, *Mater. Res. Bull.* **9,** 555 (1974).
15. E. A. Giess, J. E. Davies, and C. F. Guerci, *Mater. Res. Bull.* **10,** 355 (1975).
16. J. E. Davies, E. A. Giess, and J. D. Kuptsis, *J. Mater. Sci.* **10,** 589 (1975).
17. R. Ghez and E. A. Giess, *Mater. Res. Bull.* **8,** 31 (1973).
18. W. A. Bonner, *Mater. Res. Bull.* **9,** 885 (1974).
19. W. A. Bonner, *Mater. Res. Bull.* **10,** 15 (1975).
20. S. L. Blank, J. W. Nielsen, and W. A. Biolsi, *J. Electrochem. Soc.* **123,** 856 (1976).
21. D. C. Fowlis and J. A. Copeland, *American Institute of Physics Conference Proceedings*, No. 5, 240 (1971).
22. A. A. Thiele, *Bell Syst. Tech. J.* **48,** 3287 (1969).
23. T. Kasai and F. Ishida, *Mater. Res. Bull.* **10,** 807 (1975).
24. B. S. Hewitt, R. D. Pierce, S. L. Blank, and S. Knight, *IEEE Trans. Magnetics* **MAG-9** (1973).
25. G. G. Sumner and W. R. Cox, *American Institute of Physics Conference Proceedings*, No. 34, 157 (1976).

Received March 21, 1977; revised January 23, 1978

The author is located at the IBM General Products Division laboratory, San Jose, California 95193.